IEEE Access
Multidisciplinary | Rapid Review | Open Access Journal

Received June 26, 2019, accepted July 17, 2019, date of publication July 25, 2019, date of current version September 9, 2019.

Digital Object Identifier 10.1109/ACCESS.2019.2931366

Experimental Investigation on the Thermal Performance of a Sintered Flexible Woven Heat Sink

YONG TANG, LONGHUA DUAN, XINRUI DING, KAIHANG CHEN, GONG CHEN, BINHAI YU, AND ZONGTAO LI

Key Laboratory of Surface Functional Structure Manufacturing of Guangdong High Education Institutes, South China University of Technology, Guangzhou 510640, China

Corresponding author: Xinrui Ding (dingxr@scut.edu.cn)

This work was supported in part by the National Natural Science Foundation of China under Grant 51805173 and Grant 51735004, in part by the Science and Technology Program of Guangzhou under Grant 201904010252, in part by the Natural Science Foundation of Guangdong Province under Grant 2014A030312017, and in part by the Fundamental Research Funds for the Central Universities under Grant 2018MS44.

ABSTRACT A novel flexible woven heat sink (FWHS) composed of sintered copper braided belts was proposed here to meet the heat dissipation requirements of the flexible radiator installed in a narrow space. The sintering treatment was employed to ameliorate the tensile and bending properties as well as the thermal conductivity of the FWHS. The thermal resistance network model and the temperature field analysis in cases of natural convection and forced convection were presented to evaluate the thermal performance of the FWHS. The results show that the FWHS sintered at 850 °C with the expanded shape at a compressed height of 55 mm can reduce the temperature of heat source by 17.1% compared to the uncompressed FWHS, which demonstrates its outstanding advantage of maintaining high efficiency of heat dissipation under compressive deformation.

INDEX TERMS Flexible woven heat sink, sintered copper braided belts, forced convection, compressive deformation, heat dissipation.

I. INTRODUCTION

In recent years, electronic devices are gradually developing towards integration, high power and miniaturization, which gives rise to the dramatic increase in their power density and heat flux density [1], [2]. It is worth noting that more than 55% of the failure of diverse electronic devices is caused by the high working temperature exceeding the limit values [3]. In addition, the extreme working temperature will also lead to the decreased life expectancy of electronic or photonic products [4]–[7]. Therefore, it is crucial to adopt corresponding thermal control solutions for solving the severe heat dissipation problems [8]–[14].

Plate-fin heat sinks [15], [16] is a typical natural convection heat exchanger that have been widely used owing to its simple structure, easy processing and high heat transfer efficiency. However, the conventional finned heat sinks are not suited in heat dissipation applications with high heat flux density due to their limited surface area. Increasing the external area of the finned radiator is the preferred scheme for better heat dissipation capability, but the entire radiator will become larger and bulky with more metal consumption. Some researchers employ porous metal materials such as metal foams and metal braids to manufacture finned heat sinks with light weight and small size. Metal foams possess good heat transfer and heat dissipation capacity as well as permeability due to their unique skeleton structure [17], [18], which have been applied to many heat-exchange occasions [19]–[21]. Nevertheless, the brittleness and insufficient mechanical strength of metal foams have limited their applications in finned heat sinks.

With the shortcomings of the fixed size, heavy mass and insufficient heat dissipation capability, the conventional rigid heat sink cannot be well adapted to the application scenes with complex structure and small space. Recently, flexible heat sinks have received much attention. Metal braided materials are the promising candidate for fabricating flexible heat

The associate editor coordinating the review of this article and approving it for publication was Jiajie Fan.

sinks due to their outstanding heat transfer capability, good adaptability, high flexibility and low production cost, which have been widely used in industrial filtration, Stirling engine regenerators and aerospace [22], [23]. In addition, braided materials also provide good mechanical properties. It is found that the raw materials of fibers and the matrix, the braiding structure and braiding angle have a significant influence on the mechanical properties of braided materials [24], [25]. Carey established a numerical model to analyze the elastic modulus of two-dimensional braided materials and verified its validity for stiffness critical applications [26]. However, there is few research focused on the methods to enhance the mechanical properties of braided materials.

Moreover, metal wire mesh with porous structures are also attracting renewed interests for their large potential in heat transfer. Xu and Wirtz [27] proposed a woven mesh consisting of plain-weave conductive screens that have a highly anisotropic thermal conductivity vector, with in-plane effective thermal conductivities ranging up to 78.5% of the base material values, which is much higher than other porous media. Zhao *et al.* [28] presented a new methodology to calculate the volumetric porosity, specific surface area, and in-plane thermal conductivity for porous structures made of square-shaped and diamond-shaped wire screens. Analytical models were developed accordingly and the analysis demonstrated the good heat transfer ability of the wire mesh.

To further improve the heat transfer performance, researchers have investigated the effects of sintering on metal woven materials. Liu *et al.* [29] studied the heat transfer characteristics of sintered metal woven wire mesh with different porosity and electrically heated the sintered wire mesh structure. The results showed that the porosity of the sintered metal woven wire mesh has a great impact on the Nusselt number, and the Nusselt number changes synchronously with the fluid Reynolds number. Li and Peterson [30] conducted an experimental study on the thermal conductivity of sintered woven wire mesh. It was indicated that for a single-layer in-line structure and a multi-layer interlaced structure, the effective thermal conductivity along the normal direction is 4% $\sim$ 25% and 6.4% $\sim$ 35% of the corresponding solid metal, respectively. Apart from the intrinsic thermal conductivity of the base material, the contact state between braided wires and layers is another important factor affecting the effective thermal conductivity of the screen.

In this paper, a novel flexible woven heat sink (FWHS) was fabricated with sintered copper braided belts, which can be folded and compressed freely. The sintering temperature has been investigated to obtain superior mechanical properties and thermal conductivity of the copper braided belts. The thermal performance of the FWHS are systematically studied under different input power, as well as varying degrees of compressive deformation. Meanwhile, the heat dissipation characteristics of the flexible radiator are also tested under natural convection and forced convection conditions at various wind speeds.

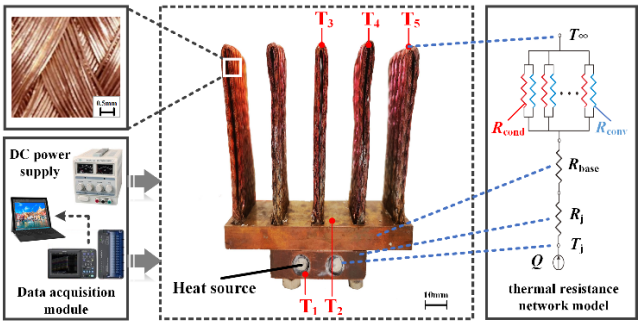

FIGURE 1. Schematic illustration of the experimental setup and the thermal resistance network model.

II. EXPERIMENTS

A. THE CONSTRUCTION OF FWHS

The sintered FWHS designed in this paper is composed of five folded sintered copper braided belts with a height of 60 mm, which are arranged in parallel arrays with a constant spacing of 12 mm on a copper substrate, as shown in Figure 1. Each copper braided belt has 24 strands, and each strand contains 12 copper wires with a diameter of 0.15 mm. The copper wires are wove in two directions with a braiding angle of 45°, forming a twill weave structure. The initial length, width and thickness of the copper braided belts are 120 mm, 30 mm and 2 mm, respectively. Each copper braided belt is folded in half with two layers and welded in the grooves (a depth of 1 mm) of the copper substrate. The dimensions of the copper substrate is 80 × 35 × 6 mm and the overall height of the FWHS is 75 mm.

B. EXPERIMENTAL SETUP

The temperature acquisition module consists of a DC stabilized power supply (SW1800X, 60 V, 5 A) for adjusting the input power of the heating rods, a computer and a data acquisition card for monitoring and recording the temperature variation. The heating block comprises a copper block with the dimension of 40 × 35 × 10 mm and two heating rods. The measured values of five K-type thermocouples for acquiring the transient temperature of the test apparatus are labeled as T1-T5. The positions of thermocouples (see Figure 1) are located at the heating rod (T1), the junction between the copper base and the copper braided belt (T2), and the end of three braided belts from the middle to the edge (T3, T4, T5). T1 is determined as the temperature of heat source to judge the heat dissipation performance of FWHS. Since the temperature values of T3, T4 and T5 are very close to each other, the mean value of T3, T4 and T5 is defined as T_m to represent the temperature at the end of the copper braided belts. The heating block and the copper base of the FWHS were wrapped by the adiabatic elastomeric foam to reduce the thermal loss during the test process. As a contrast, the thermal performance of the original FWHS using copper braided belts without any sintering treatment is also tested under the same conditions.

The experimental uncertainty is mainly the random errors occurring in the temperature measuring process.

The accuracy of the K-type thermocouple is 0.1 °C. The resolution of the data acquisition card (HIOKI-LR8510) is 0.05 °C, and the tolerance of the DC stabilized power supply is 0.5 W. All tests were carried out at 25 °C.

III. THERMAL RESISTANCE ANALYSIS

Thermal resistance is an important technical index evaluating the thermal characteristics of electronic devices [31]. Figure 1 displays the thermal resistance network model of the flexible braided radiator. The total thermal resistance (R_{tot}) of the FWHS system derives from the heating rod (R_j), the copper substrate (R_{base}), as well as the heat conduction resistance (R_{cond}) and the convective heat transfer resistance (R_{conv}) belonging to the copper braided belts. The theoretical formulas for calculating the thermal resistance are as follows:

$$R_{tot} = R_j + R_{base} + \frac{R_{cond} \times R_{conv}}{R_{cond} + R_{conv}} \quad (1)$$

$$R_{cond} = \frac{T_{s1} - T_{s2}}{Q \cdot \eta} \quad (2)$$

$$R_{conv} = \frac{1}{h \cdot A} \quad (3)$$

From Eq. (2), T_{s1} is the average temperature at the bottom (close to the heating block) and T_{s2} is the average temperature at the top (away from the heating block) of the copper braided belts (°C). Q is the input power of the DC power supply (W). The conversion coefficient (η) from the input power to thermal power is about 95%. While in Eq. (3), h is the convective heat transfer coefficient of air ($W \cdot m^{-2} \cdot K^{-1}$) and A is the surface area of one copper braided belt (m^2).

The relationship between the temperature and the total thermal resistance of the system is as follow:

$$T_j - T_\infty = Q \cdot \eta \cdot R_{tot} \quad (4)$$

where T_j is the temperature of the heating copper block (°C) and T_∞ is the ambient temperature (°C) around the radiator.

IV. RESULTS AND DISCUSSION

A. BASIC CHARACTERISTICS OF THE SINTERED COPPER BRAIDED BELTS

Different sintering process parameters have a significant impact on the mechanical and thermal properties of copper braided belts, and also affect the overall performance of the assembled flexible braided radiators subsequently [32]–[35]. In this section, the tensile and bending properties, as well as the thermal conductivity of the sintered copper braided belts under different sintering temperatures are explored, so as to determine the optimum preparation parameters of the FWHS. The thermal insulation time at all sintering temperatures is set for 1 h. The dimensions of the test samples are 100 × 30 × 2 mm.

The tensile tests were performed on a universal testing machine (ZWICK BT1-FR010TH A50, German). As illustrated in Figure 2(a), the copper braided belts were fixed by the upper and lower clamps with the same clamping length of 30mm. The upper clamp stretched the samples

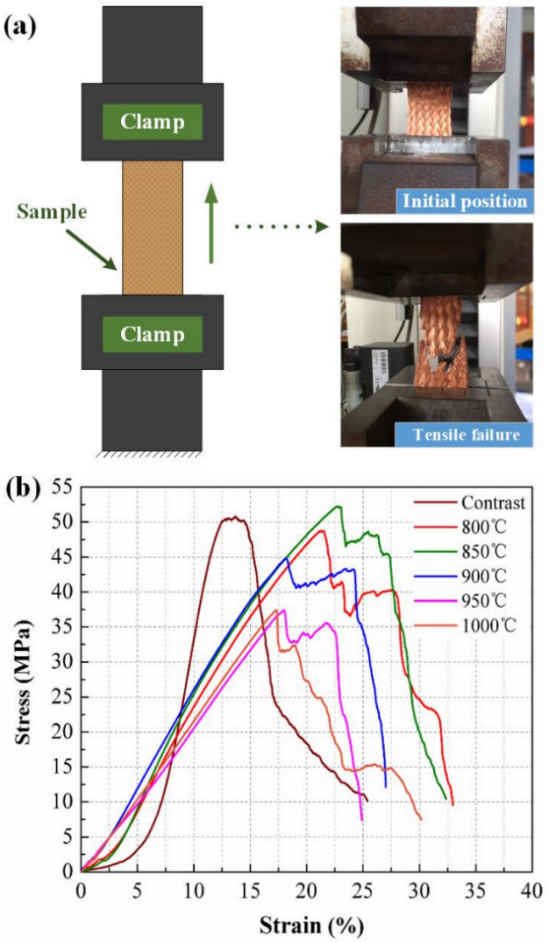

FIGURE 2. (a) The schematic of the tensile test setup. (b)Tensile stress-strain curves of copper braided belts at different sintering temperatures.

upwards at a constant rate of 5 mm/min until tensile failure occurred. Figure 2(b) depicts the tensile stress-strain curves of copper braided belts sintered at a temperature range of 800 ∼ 1000 °C. Except for the curve of the original copper braided belt without sintering treatment (labeled as "Contrast"), the variation trends in the tensile stress-strain curves of sintered braided belts at different sintering temperatures are basically similar. Evidently, all sintered samples can undergo larger strain than the contrast sample when reaching the maximum tensile stress. As presented in Figure 4(a), the maximum tensile stress and the corresponding strain of the contrast sample are 50.77 MPa and 13.7%, while the maximum tensile stress of the sintered samples is attained at 850 °C with a value of 52.22 MPa and the strain is 22.8%. This result can be attributed to the formation of sintering necks during the sintering process, which renders closer contact of copper fibers and thereby enhances the overall bonding strength of the braided belts. When undergo heat treatment at higher temperatures, the contact between copper fibers is stronger [29] and the fabrics become more rigid, which reduces the tensile toughness.

The bending tests were conducted on a universal electronic testing machine (Shimadzu AGS, Japan) with the bending

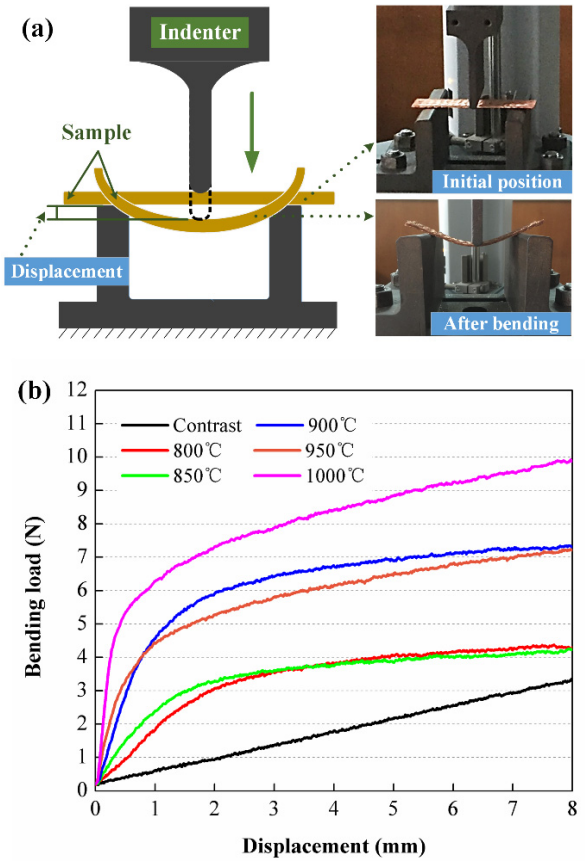

FIGURE 3. (a) The schematic of the bending test setup. (b) Bending load-displacement curves of copper braided belts at different sintering temperatures.

displacement range of 0 ∼ 8 mm. As illustrated in Figure 3(a), the flat copper braided belts were placed on the test setup without fixed restraint like a simply supported beam. The indenter initially applied a preloading force of 0.2 N to make contact with the samples and then gradually pressed downward at a constant rate of 1 mm/min until the displacement reached 8 mm.

Figure 3(b) presents the bending load-displacement curves of copper braided belts at different sintering temperatures, and the relevant bending stress of the samples at the displacement of 8 mm is shown in Figure 4(b). Under the same displacement, the original copper braided belt without sintering treatment (labeled as "Contrast") endures less bending load than the sintered braided belts and exhibits better flexibility. Moreover, the bending loads of sintered samples at different sintering temperatures rise rapidly when the displacement is below 1 mm, and then become steady as the displacement continues to increase. When the displacement reaches 8 mm, the bending load and the corresponding bending stress of the contrast sample are 3.34 N and 6.51 MPa, while the two values of sintered samples are 4.30 N, 8.39 MPa (800 °C) and 4.89 N, 9.54 MPa (850 °C), respectively. The bending stress grows with increasing sintering temperature, which indicates that the sintering treatment at higher temperature reduces the flexibility of the copper braided belts. It is primarily because tighter and firmer connection between copper fibers may form at higher temperatures, thereby increasing the overall stiffness of copper braided belts.

The thermal conductivity of copper braided belts has a direct impact on thermal control performance of the FWHS. Therefore, the thermal conductivity was measured by the thermal conductivity meter (Hotdisk-TPS). The test results are shown in Figure 4(c). Compared to the contrast sample without sintering, the thermal conductivity of sintered copper braided belts is remarkably improved. With the increase of the sintering temperature, the thermal conductivity of sintered braided belts increases first and then decreases. The maximum value obtained at 900 °C is 32.10 W/ (m·K) with an increased percentage as high as 38.7%, in comparison with 23.15 W/ (m·K) of the contrast sample. Appropriate heat treatment can promote the stable formation of sintering necks and improve the bonding degree between copper fibers, thereby enhancing the thermal conductivity of fabrics. Instead, excessive sintering temperature may lead to grain coarsening, aggravated oxidation of the grain boundary or melting of partial copper fibers, which reduces the thermal conductivity of copper fabrics.

The variation of microstructures were observed on the scanning electron microscope (SEM, Hitachi S-3700N, Japan). As shown in Figure 4(e), the original copper braided belt without heat treatment has a loose structure, in which the copper fibers are not in close contact with each other. By contrast, in Figure 4(f) the copper braided belt sintered at 850 °C demonstrates a more compact morphology. Sintering necks are formed due to the partial melting of copper fibers during the heating process, The tensile strength, bending stiffness as well as the thermal conductivity of the braided belts were therefore enhanced through the tight sintered connection.

In order to improve the tensile strength and maintain the flexibility of the copper braided belts, and meanwhile increase the thermal conductivity with relatively low sintering temperature to reduce the production cost, the above test results are comprehensively considered. The evaluation formula is introduced here:

$$f = (F \times W) / (T \times N) \tag{5}$$

where f is the synthetic evaluation factor, F is the tensile stress, W is the thermal conductivity, T is the sintering temperature and N is the bending stress. According to the calculated values in Figure 4(d), f reaches the maximum value at 850 °C. Therefore, the sintered FWHS adopted in the following experimental study is fabricated with the copper braided belts sintered at the optimum temperature of 850 °C. Besides, the sintering parameters can be determined in other ways to satisfy the needs of different applications.

B. EFFECTS OF COMPRESSIVE DEFORMATION ON THE HEAT TRANSFER PERFORMANCE OF FWHS

One significant characteristic of the copper braided belt is the excellent flexibility, making it easy to be turned, folded and compressed. Accordingly, the structural forms and external

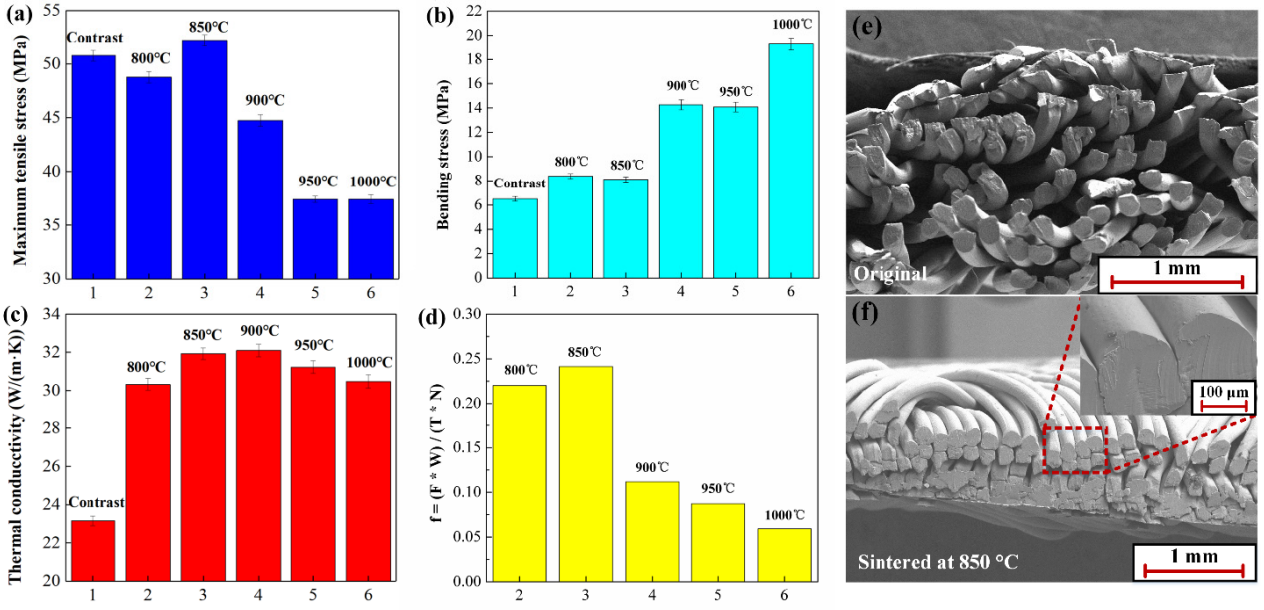

FIGURE 4. Basic characteristics of copper braided belts at different sintering temperatures: (a) the maximum tensile stress; (b) the bending stress at the displacement of 8 mm; (c) the thermal conductivity; (d) the synthetic evaluation factor; SEM images of (e) the original copper braided belt; (f) the copper braided belt sintered at 850 °C demonstrating the sintering necks.

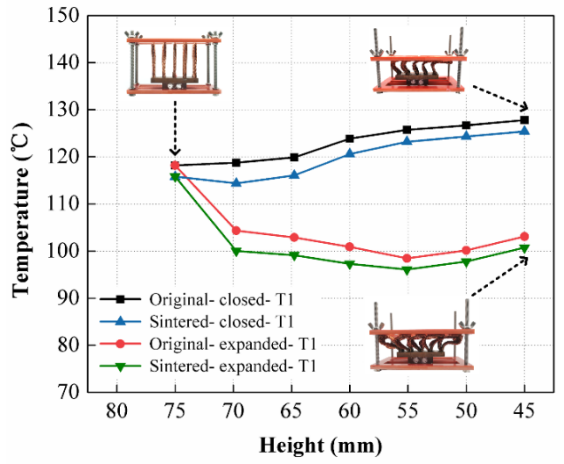

FIGURE 5. Diagram of the relationship between the equilibrium heat-source temperature (T1) and the compressed height of FWHS.

shapes of the FWHS can be adjusted expediently to adapt to the complex working environment. Figure 5 reveals the relationship between the equilibrium heat-source temperature (T1) and the compressed height of the flexible radiator in two cases of compressive deformation. In the legend, ''original'' and ''sintered'' refer to the original FWHS and the sintered FWHS, while ''closed'' and ''expanded'' refer to the compressed states of copper braided belts with closed and expanded shapes, respectively. The bottom plate and upper pressing plate are made of high-temperature resistant bakelite material with very low thermal conductivity and hollowed out to reduce their influence on convection heat transfer of the radiator. The compressed height can be changed by adjusting the position of the upper nuts on the screws. The overall height of FWHS was gradually compressed from an initial height of 75 mm to 45 mm. The input power is 25 W.

It can be observed that T1 of both the original and sintered FWHS increase continuously in the closed compression state. When the compressed height is changed from 75 mm to 45 mm, T1 of the closed sintered FWHS rises from 115.8 °C to 125.4 °C with a growth rate of 8.3%. In contrast, T1 of the closed original FWHS is 3 ∼ 5 °C higher than that of the closed sintered FWHS at any compressed height. For the compressed FWHS with closed shape, the spacing between adjacent copper braided belts changes little when the deformation is small. The situation of thermal boundary layers is similar to that of the uncompressed state, and thus small deformation of the closed compressed braided belts have little effect on the convective heat transfer of the radiator.

In another aspect, T1 of both the original and sintered FWHS in the expanded compression state decline sharply at first and then rise slightly. When the compressed height is changed from 75 mm to 55 mm, the expansion of copper braided belts greatly increases the heat dissipation area, causing T1 of the expanded sintered FWHS decline from 115.8 °C to 96.1 °C with a percentage of 17.1%. However, when compressed from 55 mm to 45 mm, T1 of the expanded sintered FWHS rises slightly from 96.1 °C to 100.7 °C. By comparison, T1 of the expanded original FWHS is 3 ∼ 6 °C higher than that of the expanded sintered FWHS at any compressed height. As the deformation degree of the radiator further increases, the spacing between adjacent copper braided belts decreases and the belts even come into contact with each other, which decreases heat dissipation area. Furthermore, the thermal boundary layers of the braided belts interfere with each other, resulting in the decreased convective heat transfer

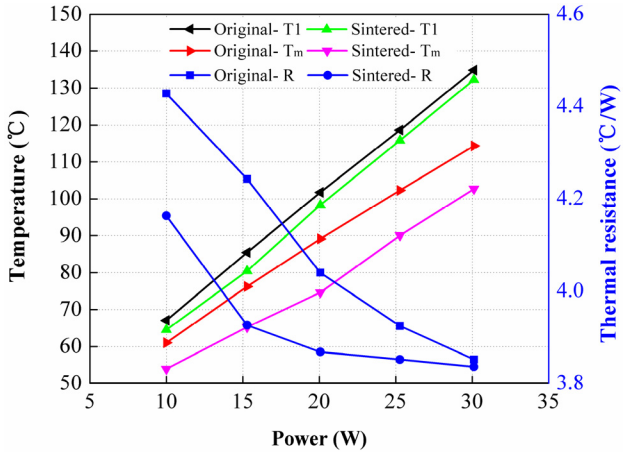

FIGURE 6. The plots of the equilibrium temperature (T1, T_m) and total thermal resistance of the original FWHS and sintered FWHS at different power levels.

capacity of FWHS. Thereby, the effect of heat accumulation increases the overall equilibrium temperature of the radiator.

It is concluded that the sintered FWHS shows better heat dissipation performance than the original FWHS in both two compressive deformation states, which benefits from the improved thermal conductivity of sintered copper braided belts. More importantly, the external shapes of the FWHS has a significant influence on the thermal performance. The equilibrium temperature of heat source decrease when the FWHS is under compressive deformation with expanded shape, which confirms that the braided radiator still has good heat dissipation capacity in a proper compression state. This outstanding feature of the flexible braided radiator offers obvious advantages in heat dissipation application of electronic devices within limited space.

C. EFFECTS OF INPUT POWER ON THE HEAT TRANSFER PERFORMANCE OF FWHS

In order to explore the influence of different input powers on the heat transfer performance of FWHS, the input power is gradually increased from 10 W to 30 W with an increment of 5 W per time. Figure 6 exhibits the plots of the equilibrium temperature (T1, T_m) and total thermal resistance of the original FWHS and the sintered FWHS at different power levels. For the two flexible radiators, both the temperature of heat source (T1) and the average temperature at the end of copper braided belts (T_m) increase almost linearly with the increase of input power. When the input power is 10 W, the temperature gap between T1 and T_m of the original FWHS is 7.2 °C, while the difference enlarges to 23.8 °C at 30 W. As for the sintered FWHS, T1 is 2 ∼ 3 °C and T_m is 8 ∼ 10 °C lower than that of the original FWHS at all power levels, respectively. Consequently, the sintered FWHS exhibits better heat dissipation capability than the original FWHS. It is also noteworthy that the temperature gaps between T1 and T_m of both the original FWHS and the sintered FWHS only increase slightly as the power increases,

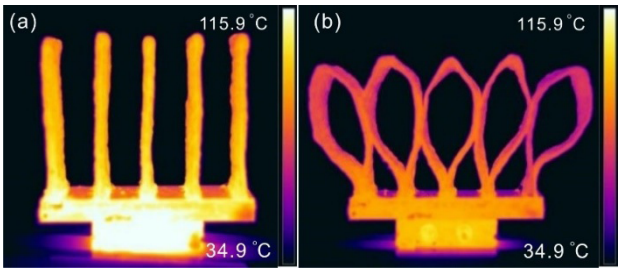

FIGURE 7. Infrared images of the sintered FWHS at thermal equilibrium (input power of 25 W) with (a) original vertical shape and (b) expanded shape by compressive deformation.

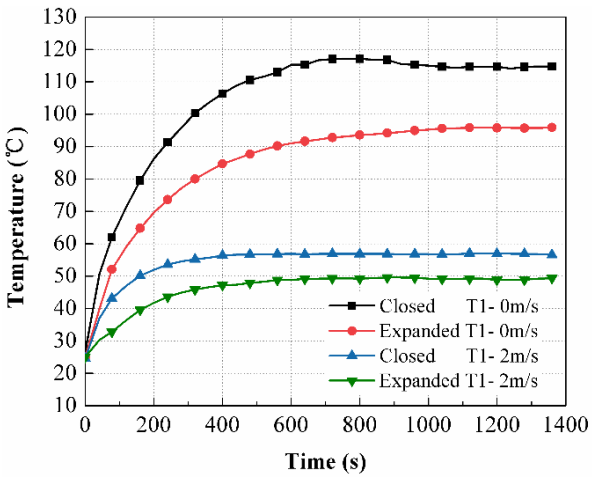

FIGURE 8. The heat-source temperature (T1) curves of the compressed sintered FWHS affected by forced air cooling.

which proves that they still maintain good thermal conductivity at higher input power. Nevertheless, the insufficient heat transfer capacity in natural convective state limits the overall heat dissipation performance of the flexible radiators, resulting in the higher temperature difference between T1 and T_m, and also the higher overall temperature.

The thermal resistance of FWHS under different input power is further analyzed. As presented in Figure 6, the total thermal resistance of the two radiators decreases with the increase of input power. Since the input power increases, the heat dissipation effect of the copper braided belts is enhanced, which leads to the gradual decline in total thermal resistance of the radiators. Besides, the gap of thermal resistance between the original FWHS and the sintered FWHS diminishes as the power increases. On account of a more compact fabric structure, the volume porosity of the sintered copper braided belts decreases, which improves the thermal conductivity, as validated by Liu *et al.* [29]. This results in lower total thermal resistance of the sintered FWHS than that of the original FWHS. Regarding lower input power, heat conduction plays a major role in heat transfer with relatively low overall temperature of radiators. However, as the input power increases, the overall temperature of both the original FWHS and the sintered FWHS continues to rise. Owing to a larger contact surface area with air of the looser fabric structure, the convective heat transfer capacity of the original

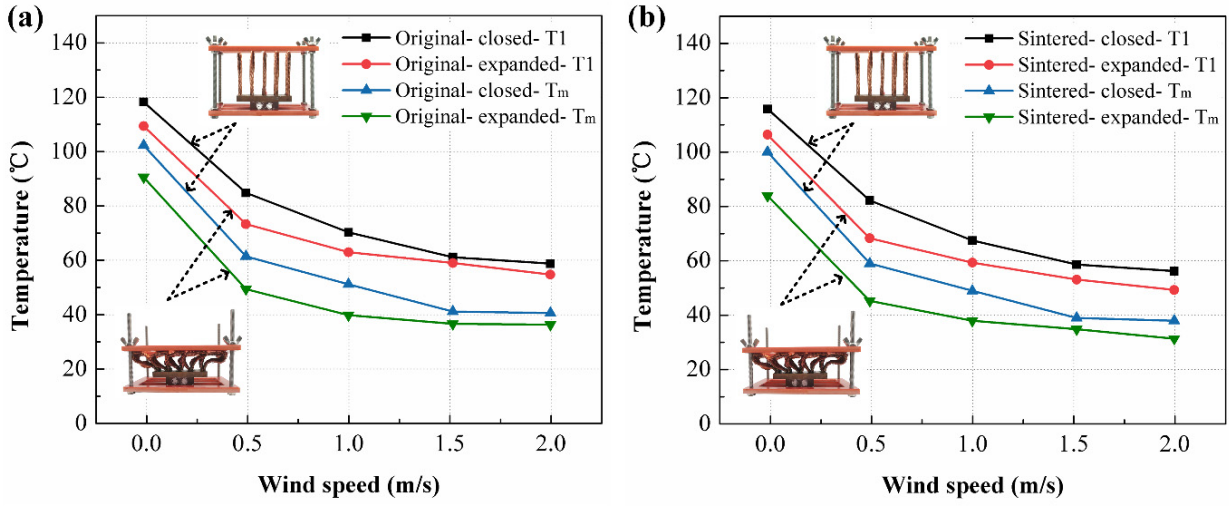

FIGURE 9. Equilibrium temperature profiles (T1, T_m) of the compressed FWHS under different wind speeds: (a) original FWHS and (b) sintered FWHS.

FWHS is higher than that of the sintered FWHS. Therefore, the gap of thermal resistance between the original FWHS and the sintered FWHS gradually decrease. Specifically, the total thermal resistance of the original FWHS and the sintered FWHS are 4.43 °C/W and 4.16 °C/W at the input power of 10 W. When the input power is up to 30 W, the total thermal resistance of the original FWHS and the sintered FWHS decrease to 3.85 °C/W and 3.83 °C/W, respectively. This can be ascribed to the constant heat transfer surface area of copper braided belts of the two radiators, which limits the convective heat transfer between the braided belts and the surrounding air flow. Hence, there is no obvious difference in the thermal resistance between the original FWHS and the sintered FWHS at high input power.

Figure 7 displays the infrared images of two sintered FWHS that have reached thermal equilibrium at the input power of 25 W. According to the temperature field of the two heating blocks and radiators, it is clear that the heat transferred from heat source is evenly distributed on the copper substrates and copper braided belts under the function of convective heat transfer with the surrounding air flow. More importantly, the overall temperature of the sintered FWHS with expanded shape by compressive deformation is evidently lower than that of the sintered FWHS with original vertical shape, which is consistent with the results in Figure 6.

D. EFFECTS OF WIND SPEED ON THE HEAT TRANSFER PERFORMANCE OF FWHS

Forced convective heat transfer is a common cooling technique that uses a fan or pump to drive the air or working fluid to flow through the heating surface and then take away the heat. Compared with the natural convection, forced convection can dramatically improve the efficiency of convective heat transfer by 10 times nearly [36]. Therefore, simple forced air cooling by a DC-powered fan is employed here to investigate the effects of wind speed on the forced convective heat transfer performance of FWHS. The input power is set at 25 W.

Figure 8 shows the heat-source temperature (T1) curves of the compressed sintered FWHS affected by forced air cooling. According to Figure 5, T1 of the expanded sintered FWHS reaches the minimum at the compressed height of 55 mm. Thereby, considering the best heat dissipation performance, the overall height of the FWHS under compressive deformation is fixed at 55 mm to study the effect of forced air cooling. There is extremely distinct difference in the curves. With the assistance of forced air cooling (the wind speed of 2 m/s), T1 of the expanded sintered FWHS at thermal equilibrium can be reduced to 49.4 °C, while T1 is as high as 95.9 °C in natural convection (the wind speed of 0 m/s). In addition, T1 of the closed sintered FWHS at thermal equilibrium decreases to 56.6 °C with forced air cooling, compared to 114.7 °C in natural convection. Moreover, it only takes about 420 s for the heat source of the expanded sintered FWHS to reach thermal equilibrium at the wind speed of 2.0 m/s, which is about 560 s shorter than that in natural convection, demonstrating the prominent efficiency of forced convective heat transfer.

It is easy to understand that the opening angle at the fold in half of the braided belts can also has an influence on the heat dissipation performance of the flexible radiator. Chen *et al.* [37] studied the structural parameters of a flexible braided radiator and found that the optimum opening angle of braided belts ranged from 25° to 40°. In this section, the equilibrium temperature (T1, T_m) of FWHS in compressed states with closed and expanded shapes are further compared under different wind speeds. Concerning better thermal performance, both the original FWHS and the sintered FWHS were tested under the compressed height of 45 mm, and the corresponding opening angle of the copper braided belts was close to 30° at this height.

As illustrated in Figure 9(a), when the wind speed is 0 m/s, T1 and T_m of the expanded original FWHS are 3.0 °C and 5.0 °C lower than that of the closed original FWHS, respectively. This can be ascribed to the stronger thermal radiation to ambient air by a larger contact area of the expanded FWHS. At the wind speed of 0.5 m/s, T1 and T_m of the expanded original FWHS are 12.0 °C and 11.0 °C lower than that of the closed one. Such great difference is due to the enhanced convective heat transfer capability of copper braided belts under the action of forced air cooling. The temperature gaps decrease to 8.0 °C (T1) and 10.0 °C (T_m) between the closed and the expanded original FWHS when the wind speed is up to 1.0 m/s. As the wind speed increases to 1.5 m/s and 2.0 m/s, the temperature gaps further narrow to 4.0 °C (T1) and 3.0 °C (T_m). This phenomenon is mainly because the advantage of thermal radiation relying on the contact area of radiators is no longer obvious at high wind speed, while the forced air cooling plays a dominant role in convective heat transfer.

V. CONCLUSION

A novel flexible radiator has been fabricated to satisfy the heat dissipation demands of electronic devices with high power density and compact inner space. The FWHS is composed of sintered copper braided belts which possess a twill weave structure and are fixed on a copper substrate. The optimal sintering temperature is selected as 850 °C for the copper braided belts to improve the mechanical and thermal conductivity. The thermal performance of the FWHS under compressive deformation and forced convection heat transfer is investigated. Results show that the sintered FWHS has better heat dissipation performance than the original FWHS owing to the higher thermal conductivity. The equilibrium time and temperature of the FWHS are significantly decreased with the assistance of forced air cooling. More importantly, the FWHS sintered at 850 °C with the expanded shape at a compressed height of 55 mm can reduce the temperature of heat source by 17.1% compared to the uncompressed FWHS, which demonstrates its outstanding advantage of maintaining high efficiency of heat dissipation under compressive deformation. It is believed that the FWHS with great flexibility and adjustability provides a new idea for cooling designs.

REFERENCES

[1] S. V. Garimella, A. S. Fleischer, J. Y. Murthy, A. Keshavarzi, R. Prasher, C. Patel, S. H. Bhavnani, R. Venkatasubramanian, R. Mahajan, Y. Joshi, B. Sammakia, B. A. Myers, L. Chorosinski, M. Baelmans, P. Sathyamurthy, and P. E. Raad, "Thermal challenges in next-generation electronic systems," *IEEE Trans. Compon. Packag. Technol.*, vol. 31, no. 4, pp. 801–815, Dec. 2008.

[2] Y. Cai, D. Liu, F.-Y. Zhao, and J.-F. Tang, "Performance analysis and assessment of thermoelectric micro cooler for electronic devices," *Energy Convers. Manage.*, vol. 124, pp. 203–211, Jul. 2016.

[3] C. M. Tan and G. Zhang, "Overcoming intrinsic weakness of ULSI metallization electromigration performances," *Thin Solid Films.*, vols. 462–463, pp. 263–268, May 2004.

[4] J.-S. Li, Y. Tang, Z.-T. Li, X.-R. Ding, L.-S. Rao, and B.-H. Yu, "Effect of quantum dot scattering and absorption on the optical performance of white light-emitting diodes," *IEEE Trans. Electron Devices*, vol. 65, no. 7, pp. 2877–2884, Jul. 2018.

[5] Y. Tang, H. Lu, J. Li, Z. Li, X. Du, X. Ding, and B. Yu, "Improvement of optical and thermal properties for quantum dots WLEDs by controlling layer location," *IEEE Access*, vol. 7, pp. 77642–77648, Jun. 2019.

[6] Z.-T. Li, K. Cao, J.-S. Li, Y. Tang, L. Xu, X.-R. Ding, and B.-H. Yu, "Investigation of light-extraction mechanisms of multiscale patterned arrays with rough morphology for GaN-based thin-film LEDs," *IEEE Access*, vol. 7, pp. 73890–73898, Jun. 2019.

[7] Z.-T. Li, C.-J. Song, Z.-Y. Qiu, J.-S. Li, K. Cao, X.-R. Ding, and Y. Tang, "Study on the thermal and optical performance of quantum dot white light-emitting diodes using metal-based inverted packaging structure," *IEEE Trans. Electron Devices*, vol. 66, no. 7, pp. 3020–3027, Jul. 2019.

[8] G. Hanreich, J. Nicolics, and L. Musiejovsky, "High resolution thermal simulation of electronic components," *Microelectron. Rel.*, vol. 40, pp. 2069–2076, Dec. 2000.

[9] Y. Tang, H. Tang, J. Li, S. Zhang, B. Zhuang, and Y. Sun, "Experimental investigation of capillary force in a novel sintered copper mesh wick for ultra-thin heat pipes," *Appl. Therm. Eng.*, vol. 115, pp. 1020–1030, Mar. 2017.

[10] R. S. Downing and G. Kojasoy, "Single and two-phase pressure drop characteristics in miniature helical channels," *Exp. Therm. Fluid Sci.*, vol. 26, pp. 535–546, Jul. 2002.

[11] C. H. Amon, J. Murthy, S. C. Yao, S. Narumanchi, C. F. Wu, and C. C. Hsieh, "MEMS-enabled thermal management of high-heat-flux devices EDIFICE: Embedded droplet impingement for integrated cooling of electronics," *Exp. Therm. Fluid Sci.*, vol. 25, pp. 231–242, Nov. 2001.

[12] H. Tang, Y. Tang, Z. Wan, J. Li, W. Yuan, L. Lu, Y. Li, and K. Tang, "Review of applications and developments of ultra-thin micro heat pipes for electronic cooling," *Appl. Energy.*, vol. 223, pp. 383–400, Aug. 2018.

[13] B. Zhuang, W. Deng, Y. Tang, X. Ding, K. Chen, G. Zhong, W. Yuan, and Z. Li, "Experimental investigation on a novel composite heat pipe with phase change materials coated on the adiabatic section," *Int. Commun. Heat Mass Transf.*, vol. 100, pp. 42–50, Jan. 2019.

[14] X. Ding, M. Li, Z. Li, Y. Tang, Y. Xie, X. Tang, and T. Fu, "Thermal and optical investigations of a laser-driven phosphor converter coated on a heat pipe," *Appl. Therm. Eng.*, vol. 148, pp. 1099–1106, Feb. 2019.

[15] C. J. Shih and G. C. Liu, "Optimal design methodology of plate-fin heat sinks for electronic cooling using entropy generation strategy," *IEEE Trans. Compon. Packag. Technol.*, vol. 27, no. 3, pp. 551–559, Sep. 2004.

[16] R. Baby and C. Balaji, "Thermal optimization of PCM based pin fin heat sinks: An experimental study," *Appl. Therm. Eng.*, vol. 54, pp. 65–77, May 2013.

[17] S. Krishnan, J. Y. Murthy, and S. V. Garimella, "A two-temperature model for solid-liquid phase change in metal foams," *J. Heat Transf.*, vol. 127, pp. 997–1004, Sep. 2005.

[18] K. Boomsma and D. Poulikakos, "The effects of compression and pore size variations on the liquid flow characteristics in metal foams," *J. Fluids Eng.*, vol. 124, no. 1, pp. 263–272, 2002.

[19] W. L. Qu and I. Mudawar, "Experimental and numerical study of pressure drop and heat transfer in a single-phase micro-channel heat sink," *Int. J. Heat Mass Transf.*, vol. 45, no. 12, pp. 2549–2565, 2002.

[20] W. H. Hsieh, J. Y. Wu, W. H. Shih, and W. C. Chiuu, "Experimental investigation of heat-transfer characteristics of aluminum-foam heat sinks," *Int. J. Heat Mass Transf.*, vol. 47, no. 23, pp. 5149–5157, Apr. 2004.

[21] H. Wang, F. Wang, Z. Li, Y. Tang, B. Yu, and W. Yuan, "Experimental investigation on the thermal performance of a heat sink filled with porous metal fiber sintered felt/paraffin composite phase change material," *Appl. Energy*, vol. 176, pp. 221–232, Aug. 2016.

[22] R. A. Wirtz, J. Xu, J.-W. Park, and D. Ruch, "Thermal/fluid characteristics of 3-D woven mesh structures as heat exchanger surfaces," *IEEE Trans. Compon. Packag. Technol.*, vol. 26, no. 1, pp. 40–47, Mar. 2003.

[23] S. C. Costa, H. Barrutia, J. A. Esnaola, and M. Tutar, "Numerical study of the heat transfer in wound woven wire matrix of a Stirling regenerator," *Energy Convers. Manage.*, vol. 79, pp. 255–264, Mar. 2014.

[24] T. Bergmann, S. Heimbs, and M. Maier, "Mechanical properties and energy absorption capability of woven fabric composites under ±45 off-axis tension," *Compos. Struct.*, vol. 125, pp. 362–373, Feb. 2015.

[25] R. S. Del, L. Iannucci, and P. T. Curtis, "Experimental investigation of the mechanical properties of dry microbraids and microbraid reinforced polymer composites," *Compos. Struct.*, vol. 125, pp. 509–519, Jul. 2015.

[26] C. Ayranci and J. P. Carey, "Predicting the longitudinal elastic modulus of braided tubular composites using a curved unit-cell geometry," *Compos. B, Eng.*, vol. 41, pp. 229–235, Apr. 2010.

[27] J. Xu and R. A. Wirtz, "In-plane effective thermal conductivity of plain-weave screen laminates," *IEEE Trans. Compon. Packag. Technol.*, vol. 25, no. 4, pp. 615–620, Dec. 2002.
[28] Z. Zhao, Y. Peles, and M. K. Jensen, "Properties of plain weave metallic wire mesh screens," *Int. J. Heat Mass Transf.*, vol. 57, pp. 690–697, Feb. 2013.
[29] Y. Liu, G. Xu, X. Luo, H. Li, and J. Ma, "An experimental investigation on fluid flow and heat transfer characteristics of sintered woven wire mesh structures," *Appl. Therm. Eng.*, vol. 80, pp. 118–126, Apr. 2015.
[30] C. Li and G. P. Peterson, "The effective thermal conductivity of wire screen," *Int. J. Heat Mass Transf.*, vol. 49, pp. 4095–4105, Oct. 2006.
[31] P.-X. Jiang, M. Li, Y.-C. Ma, and Z.-P. Ren, "Boundary conditions and wall effect for forced convection heat transfer in sintered porous plate channels," *Int. J. Heat Mass Transf.*, vol. 47, pp. 2073–2083, May 2004.
[32] R. Kamiya, B. A. Cheeseman, P. Popper, and T.-W. Chou, "Some recent advances in the fabrication and design of three-dimensional textile preforms: A review," *Compos. Sci. Technol.*, vol. 60, no. 1, pp. 33–47, 2000.
[33] K.-H. Tsai, C.-L. Hwan, W.-L. Chen, and C.-H. Chiu, "A parallelogram spring model for predicting the effective elastic properties of 2D braided composites," *Compos. Struct.*, vol. 83, pp. 273–283, May 2008.
[34] O. A. Plumb and J. C. Huenefeld, "Non-darcy natural convection from heated surfaces in saturated porous media," *Int. Commun. Heat Mass Transf.*, vol. 24, pp. 765–768, Apr. 1981.
[35] M. C. Gentry and A. M. Jacobi, "Heat transfer enhancement by delta-wing vortex generators on a flat plate: Vortex interactions with the boundary layer," *Exp. Therm. Fluid. Sci.*, vol. 14, pp. 231–242, Apr. 1997.
[36] H. K. Ma and Y. T. Li, "Thermal performance of a dual-sided multiple fans system with a piezoelectric actuator on LEDs," *Int. Commun. Heat Mass Transf.*, vol. 66, pp. 40–46, Aug. 2015.
[37] S. Chen, K. Chen, Z. Li, Y. Tang, B. Zhuang, G. Zhong, and G. Liang, "Experimental investigation on the thermal performance of a light emitting diode headlamp with a flexible woven heat sink," *Appl. Therm. Eng.*, vol. 127, pp. 1215–1222, Dec. 2017.

YONG TANG received the Ph.D. degree in mechanical engineering from the South China University of Technology, Guangzhou, China, in 1994. He has more than 13 years of experience in surface coating technology and more than 11 years in optoelectronic LED packaging. He is currently a Professor with the School of Mechanical and Automotive Engineering, South China University of Technology, and the Director of the Engineering Research Center of Green Manufacturing for Energy-Saving and New Energy Technology. He is specialized in energy-saving solid-state lighting.

LONGHUA DUAN received the B.E. degree from the Department of Mechanical Engineering, Wuhan Institute of Technology, Wuhan, China, in 2017. He is currently pursuing the M.D. degree with the Key Laboratory of Surface Functional Structure Manufacturing of Guangdong High Education Institutes, South China University of Technology. His research interests include surface properties in clean energy and the high power LED devices.

XINRUI DING received the Ph.D. degree in mechanical engineering from the South China University of Technology, Guangzhou, China, in 2015. From 2015 to 2017, he joined the M.E. Department, University of California at Berkeley, as a Postdoctoral Researcher. Since 2018, he has been with the Key Laboratory of Surface Functional Structure Manufacturing of Guangdong High Education Institutes, South China University of Technology, as an Associate Professor. His current research interests include the LED packaging, optical designing, laser illumination, and semiconductor reliability.

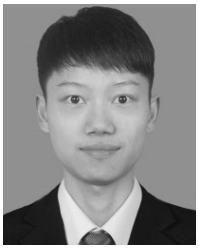

KAIHANG CHEN received the B.E. degree in mechanical engineering from the South China University of Technology, Guangzhou, China, in 2016, where he is currently pursuing the M.E. degree. His current research interests include the simulation, packaging, and application of LED.

GONG CHEN received the B.E. degree in mechanical engineering from the South China University of Technology, Guangzhou, China, in 2017, where he is currently pursuing the Ph.D. degree. His research interests include surface properties in clean energy and its high efficient usage.

BINHAI YU received the Ph.D. degree in mechanical and electronic engineering from the Huazhong University of Science and Technology, Wuhan, China, in 1997. He was the Vice Chairman of Foshan Nationstar Optoelectronics Company Ltd., Foshan, China, from 2007 to 2014. He is currently a Professor with the School of Mechanical and Automotive Engineering, South China University of Technology, Guangzhou, China. His research interests include the LED luminaire, SMD LED, high-power LED packaging, and new packaging process.

ZONGTAO LI received the Ph.D. degree in microelectronics manufacture engineering in mechanical engineering from the South China University of Technology, Guangzhou, China, in 2014. He is currently with the Engineering Research Center of Green Manufacturing for Energy-Saving and New Energy Technology, South China University of Technology, and with the Optoelectronics Engineering Technology Research and Development Center, Foshan Nationstar Optoelectronics Company Ltd., Foshan, China. His major research interests include packaging of high-power LEDs, lighting quality, and device reliability.